

WATER SORPTION AND GLASS TRANSITION OF FREEZE-DRIED CAMU-CAMU (*MYRCIARIA DUBIA* (H.B.K.) Mc VAUGH) PULP

M. A. da Silva¹, P. J. A. Sobral² and T. G. Kieckbusch^{1*}

¹Universidade Estadual de Campinas - Faculdade de Engenharia Química (FEQ/UNICAMP), 13083-970 Campinas, SP, Brazil

²Universidade de São Paulo, Faculdade de Zootecnia e Engenharia de Alimentos (FZEA/USP), 13630-000 Pirassununga, SP, Brazil

Differential scanning calorimetry (DSC) was used to determine phase transitions of freeze-dried camu-camu pulp in a wide range of moisture content. Samples were equilibrated at 25°C over saturated salt solutions in order to obtain water activities (a_w) between 0.11–0.90. Samples with $a_w > 0.90$ were obtained by direct water addition. At the low and intermediate moisture content range, Gordon–Taylor model was able to predict the plasticizing effect of water. In samples, with $a_w > 0.90$, the glass transition curve exhibited a discontinuity and T_g was practically constant (–58.8°C), representing the glass transition temperature of the maximally concentrated phase (T_g).

Keywords: camu-camu, differential scanning calorimetry, glass transition, melting

Introduction

Camu-camu is a tropical tree that grows in flooded areas of the Amazon region. The increasing consumer demand for camu-camu fruits is mainly due to its high ascorbic acid content (up to 4000 mg AA/100 g of pulp), making this fruit the richest known natural source of vitamin C [1, 2]. Despite camu-camu being commercialized only as fresh fruit in Brazil, it is interesting to note that many researches are being made in order to apply technological knowledge to obtain processed products that could be easily stored and transported [3].

Various changes in physical, chemical and biological characteristics of food stuffs occur during processing, storage and distribution. Therefore, phase transitions of foods are important in characterizing their quality and in designing efficient processing systems [4–6]. In various food products, the solids may be in an amorphous metastable state which can be formed in various processes, such as baking, concentration, freezing, freeze drying, drum drying, spray drying and extrusion, that require a sufficiently short time for removal of water or cooling of concentrated solids [7–9].

The physical state of amorphous materials may change from a solid glassy state to a liquid-like ‘rubbery’ state when the glass transition temperature (T_g) is reached. Glass transition is a second order time–temperature–moisture dependent transition generally characterized by changes in the physical, mechanical, electrical and thermal properties of the food material. It has been presumed that amorphous foods are stable in their solid,

glassy state below T_g as the molecules are kinetically immobilized in the high viscosity (10^{12} Pa s) solid glass [4, 5]. It is known that stickiness and collapse of dehydrated powdered products occurs due to a drastic decrease in viscosity above T_g [10, 11]. In the glassy state, some reactions that depend on molecular diffusion, such as chemical and enzymatic modifications, may be prevented, although this behavior does not seem to be generalized for all the chemical changes [12]. So, according to the Food Polymer Science concepts, T_g can be taken as a reference parameter to characterize product properties, quality, stability and safety of food systems. The state diagram is commonly used to identify different phase boundaries in food materials and has important applications in determining product stability during storage and in optimizing processing conditions [13]. These diagrams are able to describe the influence of food composition on stability, and show the effect of temperature and moisture content on material characteristics, allowing the product shelf life to be prolonged [7, 14]. The objective of the present work was to determine phase transitions for freeze-dried camu-camu pulp as a function of moisture content and establish the state diagram for this material.

Experimental

Camu-camu used in this work was purchased at CEAGESP (São Paulo, SP) being harvested in Southeast Brazil. The fruits were visually selected by color, size and physical damage. Only ripe fruits were used.

* Author for correspondence: theo@feq.unicamp.br

After selection, the fruits were washed in chlorinated water (10 ppm). Blanching was performed with whole fruits by immersion in hot water (98°C/2 min) followed by cooling in an ice bath for approximately 1 min. The fruits were cut in halves and the seeds were manually removed. The pulp was obtained by a domestic centrifuge (screen openings 1 mm), poured and sealed into polyethylene bags (500 g) and immediately frozen at -18°C in a vertical freezer. The frozen pulp was freeze-dried in a bench freeze-drier (EZ-DRY, FTS Systems, USA) at -50°C and 100 mTorr for 48 h. Representative samples of the fresh pulp were used to determine moisture content (vacuum drier, 95°C/100 mmHg, 48 h), ascorbic acid content by iodine titration [15], total soluble solids by refractometry (ABBE, Atago, 3T, Japan), reducing and non-reducing sugars by Fehling's method and titratable acidity [16], pectin by Carré and Haynes method [17] and pH by direct reading with a pHmeter (WTW, pH 320, Germany). All measurements were made in triplicate and the average value is reported.

Freeze-dried samples (≈ 1 g) were maintained in closed environments of constant relative humidity obtained with saturated salt solutions (LiCl, MgCl₂, K₂CO₃, Mg(NO₃)₂, NaNO₂, NaCl, (NH₄)₂SO₄, KCl, BaCl₂) at 25°C, in order to reach water activities between 0.11 and 0.90 [18]. After equilibrium was reached (about 2 weeks), samples of approximately 10 mg (± 0.1 mg) were taken for DSC analysis. After DSC analysis, the remaining material was used to determine equilibrium moisture content (vacuum oven, 95°C/100 mmHg, 48 h) and water activity at 25°C (Aqualab, CX2, Decagon Devices Inc., USA). In the high moisture content domain ($a_w > 0.90$), samples were obtained by direct addition of distilled water to the freeze-dried sample [19]. These wetted mixtures were equilibrated at 4°C for 24 h before DSC analysis.

Phase transitions were determined by differential scanning calorimetry using a DSC TA2010 controlled by a TA5000 module (TA Instruments, USA). Samples, conditioned in TA aluminum pans were heated from -120 to 120°C at a heating rate of 10°C min⁻¹ under inert atmosphere (45 mL min⁻¹ of N₂). An empty pan was used as reference. Liquid nitrogen was used for sample cooling before the runs. Samples showing devitrification peak after the first run, were annealed at the devitrification peak temperature (T_d) for 30 min before the second DSC run. Glass transition temperature (T_g), devitrification temperature (T_d), onset of ice melting temperature (T_m) and enthalpies of ice melting (ΔH_m) and devitrification (ΔH_d) were determined by the thermograms from DSC using the Software Universal Analysis V1.7F (TA Instruments). All measurements were made in triplicate. All regressions were made with the help of Software Statistica V.1.1.5 using Quasi-Newton method.

Results and discussion

Raw material

The chemical composition of fresh camu-camu pulp is presented in Table 1. The reducing sugar content was low in comparison with most fruits. Sucrose was absent, but according to Zapata and Dufour [2] this profile is typical of fruits with high ascorbic acid content. The high acidity, together with the low sugar content induces a low value of brix/acidity ratio, which is often used as an indicator of sensorial and quality characteristics.

Table 1 Chemical composition of camu-camu fresh pulp

Component	Result*
Moisture (g H ₂ O/100 g)	93.35 \pm 0.04
Total soluble solids (°Brix)	6.0 \pm 0.1
Reducing sugars (g glucose/100 g)	3.25 \pm 0.03
Non-reducing sugars (g sucrose/100 g)	ND**
Titratable acidity (g citric acid/100 g)	2.30 \pm 0.03
pH	2.63 \pm 0.02
ascorbic acid (mg AA/100 g)	1721.7 \pm 15.9
Brix/acidity ratio	2.60

*wet basis, ** not detectable

Sorption isotherm

The adsorption isotherm of freeze-dried camu-camu pulp at 25°C was obtained and is shown in Fig. 1. As observed, sample conditioning allowed the correlation of equilibrium moisture content with its respective water activity at 25°C. The sigmoidal shape of the isotherm is typical of food products and biological materials [20] and was similar to the isotherms found by Sá and Sereno [21] for strawberries, grape and onion. Guggenheim-Anderson-DeBoer (GAB) model (Eq. (1)) was used to adjust the experimental points ($r^2=0.996$).

$$X_w = \frac{CkX_m a_w}{(1 - ka_w)(1 - ka_w + Cka_w)} \quad (1)$$

In Eq. (1), X_w is the moisture content (dry basis), a_w is the water activity, X_m is the monolayer moisture content and C and k are parameters associated with the enthalpies of monolayer and multilayers, respectively [22]. The values of these parameters, calculated by non-linear regression, were $X_m=0.158$ g H₂O/g (dry basis), $C=27.364$ and $K=0.924$.

DSC experiments

In the low moisture content range ($0.11 \leq a_w \leq 0.75$), samples exhibited only one well defined glass transition represented by an endothermic deviation in the

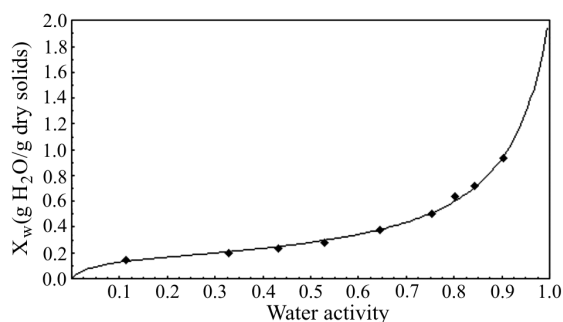


Fig. 1 Sorption isotherm of freeze-dried camu-camu pulp at 25°C

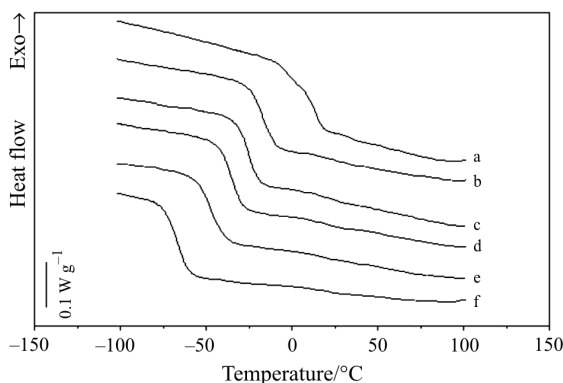


Fig. 2 DSC curves of freeze-dried camu-camu pulp in the low moisture content domain (a_w, X_w): a – 0.11, 0.128; b – 0.33, 0.166; c – 0.43, 0.189; d – 0.53, 0.217; e – 0.65, 0.276; f – 0.75, 0.334

baseline (Fig. 2). It can be observed that due to the plasticizing effect of water, T_g moved towards lower temperatures by increasing the moisture content. This same trend was observed by several authors working with other freeze-dried fruits [14, 19, 22–24].

Ice formation was observed in samples with water activities higher than 0.75. However, samples with a_w of 0.80 and 0.84 showed a devitrification peak after glass transition and before ice melting. Since T_g controls viscosity of the unfrozen material, rapid cooling of solutions may result in partial freeze-concentration and ice formation during rewarming (devitrification) above T_g of the partially freeze-concentrated solution [7, 25]. Devitrification is an exothermal transition, which results from the release of heat during ice formation. Annealing was performed in these samples by holding the sample at T_d for 30 min, allowing a maximum amount of ice to be formed and leading to a maximum concentrated solid matrix. As expected isothermal annealing led to an increase in T_g and the elimination of the devitrification exotherm. This time dependence of ice formation, which is associated with heating of rapidly cooled solutions is typical for rapidly carbohydrate solution [20]. The DSC curves for the samples before and after annealing are showed in Fig. 3.

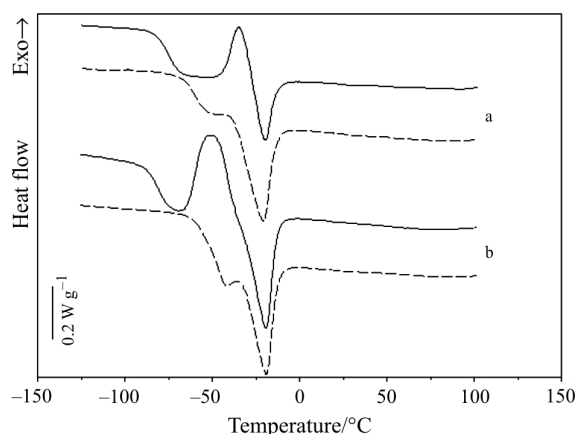


Fig. 3 DSC curves of freeze-dried camu-camu pulp in the intermediate moisture content domain (a_w, X_w): a – 0.80, 0.388; b – 0.84, 0.418; — — without annealing and --- with annealing

Thermal properties of the samples before and after annealing are showed in Table 2. The ascending T_g suggested that plasticizing water was removed from the partially freeze-concentrated solute matrix during annealing.

In the high moisture content range ($a_w > 0.90$), two thermal events between -120 and 120°C were observed (Fig. 4). The endothermic peak of ice melting was the most visible phenomenon. T_g appeared as a small deviation of the baseline before the ice melting endotherm because the heat involved in glass transition is negligible in comparison with the latent heat of ice melting [24]. In samples with high moisture content, ice formation causes freeze-concentration of dissolved solids and a decreasing in freezing temperature for the remaining water, resulting in the formation of an amorphous freeze-concentrated phase that contains unfrozen water within the ice phase [9, 26, 27]. At sufficiently low temperatures, the freeze-concentrated phase may solidify in the glassy state and ice formation ceases due to kinetic restrictions. So, for samples showing ice formation the T_g is actually the glass transition temperature of the maximally freeze-concentrated phase (T_g'). As expected, T_g' for the samples with $a_w > 0.90$ remained practically constant, independent of the moisture content (Fig. 4). For frozen

Table 2 Phase properties before and after annealing

Sample	a_w	
	0.80	0.84
Before annealing		
$T_g/^\circ\text{C}$	-74.8 ± 0.3	-80.3 ± 1.2
$\Delta H_m/\text{J g}^{-1}$	8.5 ± 2.9	31.0 ± 1.0
$T_d/^\circ\text{C}$	-33.2 ± 2.0	-52.2 ± 3.9
After annealing		
$T_g/^\circ\text{C}$	-62.7 ± 2.2	-47.5 ± 3.4

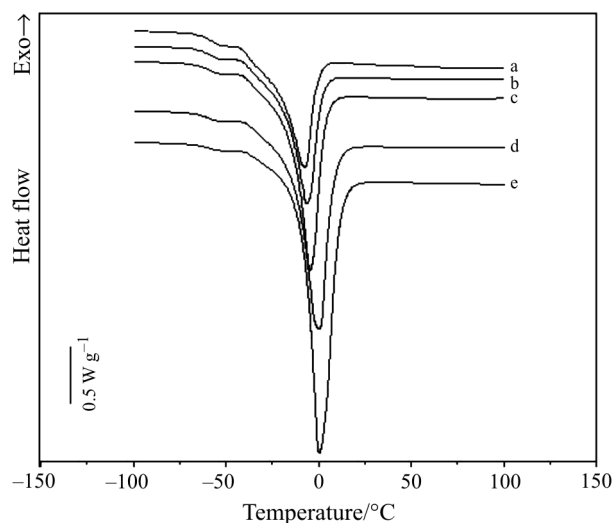


Fig. 4 DSC curves of freeze-dried camu-camu pulp in the high moisture content domain (a_w, X_w): a – 0.91, 0.538; b – 0.93, 0.586; c – 0.95, 0.638; d – 0.96, 0.693; e – 0.98, 0.791

foods, T_g' becomes the reference parameter concerning chemical and physical changes, since below T_g' diffusion limited reactions are greatly restricted. Similar results were observed by Sá *et al.* [28] with apple, Roos and Karel [8] with dilute sucrose solutions, Telis and Sobral [19] with pineapple and Moraga *et al.* [14] with strawberries.

The state diagram for freeze-dried camu-camu pulp is showed in Fig. 5. In the range of $a_w < 0.90$, the plasticizing effect of water was evident, showing a great reduction in T_g by increasing the moisture content, especially in the lower moisture content range. The Gordon–Taylor model (Eq. (2)) adequately adjust the experimental data ($r^2=0.995$). The predicted model parameters, calculated by non-linear regression were $T_{gs}=347.6$ K (74.6°C) and $K=3.92$, being T_{gs} the glass transition temperature of the anhydrous solids and K a constant. The glass transition temperature of pure water (T_{gw}) was considered 138 K (–135°C).

$$T_{g_m} = \frac{X_s T_{gs} + k X_w T_{gw}}{X_s + k X_w} \quad (2)$$

In the high moisture content range ($a_w > 0.90$), the continuous glass transition curve exhibit a sudden increase in T_g and the temperatures approached a constant value (–58.8°C), corresponding to T_g' (horizontal arrow in Fig. 5).

Figure 6 shows the DSC curve obtained for a 10 mass/mass% solution of ascorbic and citric acid (1:1.33), which is the concentration ratio normally found in camu-camu. The value of T_g' obtained for this solution (–62.9°C) suggests that the low value of T_g' observed for camu-camu pulp is mainly influenced by its

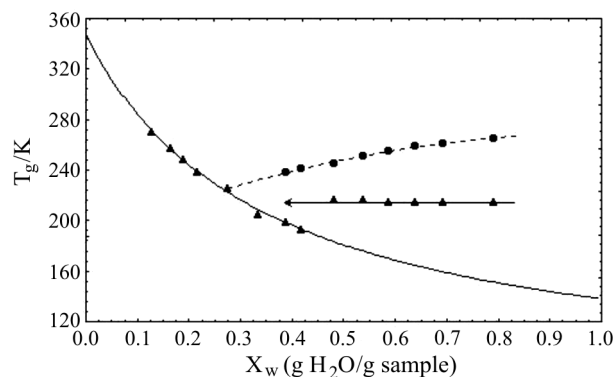


Fig. 5 State diagram of freeze-dried camu-camu pulp: \blacktriangle – T_g , \bullet – T_m

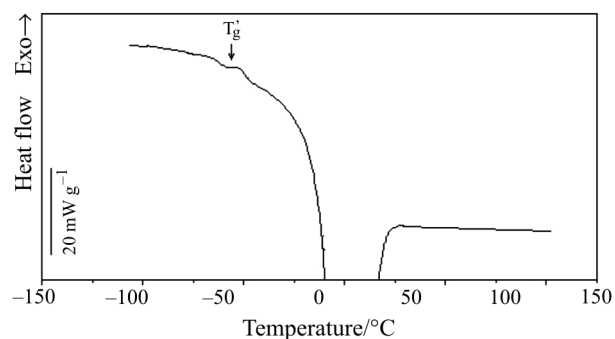


Fig. 6 DSC curve for a 10 mass/mass% solution of ascorbic and citric acid (1:1.33)

high concentration of ascorbic and citric acid and not by its sugar concentration as for most fruits [4, 19, 24].

The melting curve is also showed in the state diagram of Fig. 5. As expected the onset melting temperature (T_m), for samples showing ice melting, decreased with decreasing the moisture content. The experimental data were adjusted by a polynomial model, represented by Eq. (3) ($r^2=0.995$).

$$T_m = 186.54 + 162.58 X_w - 79.35 X_w^2 \quad (3)$$

The intersection of the glass transition and melting curves, should theoretically occur at T_g' [4, 20]. According to Eq. (3), the intersection occurs around –49.2°C, corresponding to an unfrozen water content of 0.27 g H₂O/g sample. This temperature was higher than the one obtained by the high moisture content samples (indicated by the horizontal arrow). The same behavior was observed by Telis and Sobral [29] with tomatoes. These authors attributed this difference to the lack of experimental points in this region of the diagram.

As expected, enthalpy of ice melting showed a linear dependence on moisture content (Fig. 7), represented by Eq. (4), $r^2=0.994$. Therefore, the amount of unfrozen water can be determined by extrapolation of the curve to $\Delta H_m=0$, which would represent the minimal

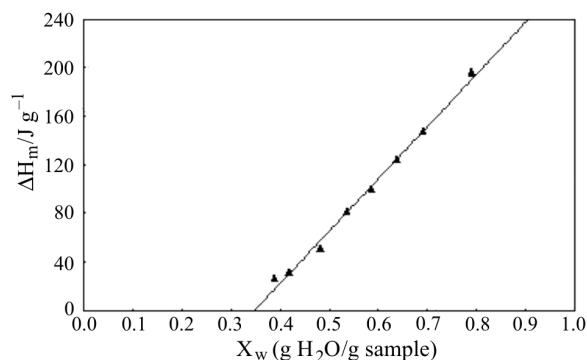


Fig. 7 Ice melting enthalpy as a function of moisture content

moisture content where ice formation is observed or X_w' [4, 23].

$$\Delta H_m = 430.47X_w - 149.76 \quad (4)$$

The unfrozen water content calculated by Eq. (4) was 0.35 g H₂O/g sample. So, T_g' can be estimated by substitution of this value in Eq. (2), resulting in a $T_g' = -67.3^\circ\text{C}$, which was considerably lower than the value observed by the samples in the high moisture content range. The same trend was observed by Telis and Sobral [19] with pineapple.

Conclusions

DSC showed to be an adequate method for the determination of phase transitions of camu-camu and therefore for the construction of the state diagram for this fruit. Devitrification peaks were observed in samples with a_w 0.80 and 0.84, which completely disappeared after 30 min of isothermal annealing at T_d . Gordon–Taylor model adjusted well the experimental points in the low and intermediate moisture content range. Samples with $a_w > 0.90$, exhibited a T_g value practically constant (-58.8°C) which represented the glass transition temperature of the maximally freeze concentrated phase (T_g'). The low value of T_g' observed for camu-camu pulp can be mainly attributed to its high concentration of ascorbic and citric acid and not only to its sugar composition, since camu-camu presented a low sugar concentration compared with other fruits.

Acknowledgements

The authors gratefully acknowledge the financial support from FAEP/UNICAMP.

References

- 1 K. C. Justi, J. V. Visentainer, N. E. Souza and M. Matsushita, *Arch. Latinoamer. Nutr.*, 50 (2000) 405.

- 2 S. M. Zapata and J. P. Dufour, *J. Sci. Food Agri.*, 61 (1993) 349.
- 3 R. B. Rodrigues, H. C. Menezes, L. M. C. Cabral, M. Dornier, G. M. Rios and M. Reynes, *J. Food Eng.*, 63 (2004) 97.
- 4 L. Slade and H. Levine, *Crit. Rev. Food Sci. Nutr.*, 30 (1991) 115.
- 5 G. W. White and S. H. Cakebread, *J. Food Technol.*, 1 (1966) 73.
- 6 A. Raemy, *J. Therm. Anal. Cal.*, 71 (2003) 273.
- 7 Y. H. Roos, *J. Food Eng.*, 24 (1995) 339.
- 8 Y. Roos and M. Karel, *J. Food Sci.*, 56 (1991) 266.
- 9 H. Levine and L. Slade, *Carbohydr. Polym.*, 6 (1986) 213.
- 10 F. P. Collares, T. G. Kieckbusch and J. R. D. Finzer, *Braz. J. Food Technol.*, 5 (2002) 117.
- 11 B. R. Bhandari and T. Howes, *J. Food Eng.*, 40 (1999) 71.
- 12 L. N. Bell and M. J. Hageman, *J. Agri. Food Chem.*, 42 (1994) 2398.
- 13 Y. H. Roos, *J. Therm. Anal. Cal.*, 71 (2003) 197.
- 14 G. Moraga, N. Martínéz-Navarrete and A. Chiralt, *J. Food Eng.*, 62 (2004) 315.
- 15 Instituto Adolfo Lutz, *Normas Analíticas do Instituto Adolfo Lutz (Vol. I)*, 3rd Ed., Instituto Adolfo Lutz, São Paulo 1985.
- 16 Association of Official Analytical Chemistry (A.O.A.C.), *Official Methods of Analysis*. Washington 1995, p. 1141.
- 17 D. Pearson, *The Chemical Analysis of Foods*, 6th Ed., J. Churchill and A. Churchill, London 1970.
- 18 W. E. L. Spiess and W. R. Wolf, in: F. Escher, B. Hallstrom, H. S. Meffert, W. E. L. Spiess and G. Voss (Eds), *Physical Properties of Foods*, Applied Science Publishers, New York 1983, p. 65.
- 19 V. R. N. Telis and P. J. A. Sobral, *Lebensm. Wiss. u- Technol.*, 34 (2001) 199.
- 20 Y. H. Roos, *Phase Transitions in Foods*, 1st Ed., Academic Press Inc., California 1995, p. 360.
- 21 M. M. Sá and A. M. Sereno, *Thermochim. Acta*, 246 (1994) 285.
- 22 V. R. N. Telis, A. L. Gabas, F. C. Menegalli and J. Telis-Romero, *Thermochim. Acta*, 343 (2000) 49.
- 23 Y. H. Roos, *J. Food Sci.*, 52 (1987) 146.
- 24 P. J. A. Sobral, V. R. N. Telis, A. M. Q. B. Habitante and A. Sereno, *Thermochim. Acta*, 376 (2001) 83.
- 25 H. D. Goff and M. E. Sahagian, *Thermochim. Acta*, 280/281 (1996) 449.
- 26 R. J. Bellows and C. J. King, *AIChE Symp. Series*, 69 (1973) 33.
- 27 Y. H. Roos, M. Karel and J. L. Kokini, *Food Technol.*, 50 (1996) 95.
- 28 M. M. Sá, A. M. Figueredo and A. M. Sereno, *Thermochim. Acta*, 329 (1999) 31.
- 29 V. R. N. Telis and P. J. A. Sobral, *Food Res. Int.*, 35 (2002) 435.

Received: May 15, 2005

Accepted: July 27, 2005

DOI: 10.1007/s10973-005-7111-z